On the growth kinetics of Ni(Pt) silicide thin films

J. Demeulemeester, D. Smeets, C. M. Comrie, N. P. Barradas, A. Vieira et al.

Citation: J. Appl. Phys. **113**, 163504 (2013); doi: 10.1063/1.4802738
View online: http://dx.doi.org/10.1063/1.4802738
View Table of Contents: http://jap.aip.org/resource/1/JAPIAU/v113/i16
Published by the American Institute of Physics.

On the growth kinetics of Ni(Pt) silicide thin films

J. Demeulemeester,[1,a)] D. Smeets,[1] C. M. Comrie,[2] N. P. Barradas,[3] A. Vieira,[4] C. Van Bockstael,[5] C. Detavernier,[5] K. Temst,[1] and A. Vantomme[1]
[1]*Instituut voor Kern- en Stralingsfysica, KU Leuven, Celestijnenlaan 200D, B-3001 Leuven, Belgium*
[2]*Department of Physics, University of Cape Town, Rondebosch 7700, South Africa*
[3]*Instituto Tecnológico e Nuclear, Estrada Nacional 10, Apartado 21, 2686-953 Sacavém, Portugal and Centro de Física Nuclear da Universidade de Lisboa, Av. Prof. Gama Pinto 2, 1699 Lisboa Codex, Portugal*
[4]*Instituto Superior de Engenharia do Porto, Rua S. Tome, 4200 Porto, Portugal*
[5]*Department of Solid State Sciences, Ghent University, 9000 Gent, Belgium*

(Received 14 August 2012; accepted 2 April 2013; published online 24 April 2013)

We report on the effect of Pt on the growth kinetics of δ-Ni_2Si and $Ni_{1-x}Pt_xSi$ thin films formed by solid phase reaction of a Ni(Pt) alloyed thin film on Si(100). The study was performed by real-time Rutherford backscattering spectrometry examining the silicide growth rates for initial Pt concentrations of 0, 1, 3, 7, and 10 at. % relative to the Ni content. Pt was found to exert a drastic effect on the growth kinetics of both phases. δ-Ni_2Si growth is slowed down tremendously, which results in the simultaneous growth of this phase with $Ni_{1-x}Pt_xSi$. Activation energies extracted for the $Ni_{1-x}Pt_xSi$ growth process exhibit an increase from $E_a = 1.35 \pm 0.06$ eV for binary NiSi to $E_a = 2.7 \pm 0.2$ eV for $Ni_{1-x}Pt_xSi$ with an initial Pt concentration of 3 at. %. Further increasing the Pt content to 10 at. % merely increases the activation energy for $Ni_{1-x}Pt_xSi$ growth to $E_a = 3.1 \pm 0.5$ eV. © *2013 AIP Publishing LLC* [http://dx.doi.org/10.1063/1.4802738]

I. INTRODUCTION

For decades, the importance of silicide contact layers in CMOS-technology has triggered major interest in the growth mechanisms and properties of silicide thin films.[1] NiSi contact films alloyed with Pt are currently applied due to Ni being the dominant diffusing species, the outstanding electrical properties, decreased silicon consumption and reduced thermal budget compared to formerly applied disilicides.[2] NiSi films are essentially grown by thermal annealing of a thin Ni film on Si(100). This results in a sequential phase formation, i.e., Ni $\rightarrow$ δ-$Ni_2Si + \theta \rightarrow$ NiSi $\rightarrow$ $NiSi_2$, in which $NiSi_2$ is a high resistivity phase that nucleates at temperatures above 800 °C.[3–5] The growth of δ-Ni_2Si and NiSi, on the other hand, is diffusion controlled with Ni as dominant diffusing species.[6–8]

The addition of Pt to the initial Ni film prior to annealing was shown to increase the thermal stability of the $Ni_{1-x}Pt_xSi$ thin film against degradation processes, such as (i) thin film agglomeration and (ii) the nucleation of high-resistive $NiSi_2$.[9–11] Recent investigations in this field focus on addressing the role of Pt in this stabilization effect. Earlier work indicated that the erratic and complex redistribution behavior of Pt during the silicide formation governs the growth properties of the solid phase reaction, even for small initial Pt concentrations.[12] More specifically, Pt appears highly concentrated in the NiSi layer in the early growth stages, affecting the texture selection. As a consequence, the $Ni_{1-x}Pt_xSi$ films exhibit a reduction of those axiotaxial texture components, which are more prone to agglomeration.[13] On the other hand, the insolubility of Pt in $NiSi_2$ compared to its solubility in $Ni_{1-x}Pt_xSi$ shifts the $NiSi_2$ nucleation towards elevated temperatures. Besides thermodynamical considerations, it has been shown that Pt has a large influence on the growth kinetics as well.[14] Alloying Ni with Pt influences the δ-Ni_2Si growth properties by forming a diffusion barrier[15] and decorating the δ-Ni_2Si grain boundaries, which constitute the dominant Ni diffusion paths.[16] Moreover, since Pt appears highly concentrated at the reaction interface during the early stages of NiSi growth, Pt can have a large effect on the $Ni_{1-x}Pt_xSi$ growth kinetics as well. Therefore, in this paper, we report on the influence of Pt addition on the growth properties of both δ-Ni_2Si and NiSi.

II. EXPERIMENTAL DETAILS

A. Sample preparation and data acquisition

Several Ni(Pt)/⟨Si⟩ alloy thin films containing a Pt concentration of 0, 1, 3, 7 and 10 at. % were prepared by simultaneous sputter-deposition of Ni and Pt in Ar plasma on Si(100) substrates. All substrates were chemically cleaned (RCA) and dipped into a 2% HF solution prior to deposition. The total metal alloy thickness is fixed at 75 nm. The reference sample without Pt is slightly thicker (85 nm) and is capped with 3 nm of Si to prevent oxidation. Real-time Rutherford backscattering spectrometry (RBS) was applied to study the solid-phase reaction, i.e., acquiring RBS spectra at periodic time intervals *in situ* during the thermal treatment of the sample. The real-time RBS experiments (and thus the annealing) were executed in vacuum better than 10^{-7} mbar while ramp-annealing the sample(s) in 2 stages. A fast ramp rate at 20 °C/min to 240 °C was used to reduce the measuring time, whereas the solid-phase reaction was captured at a slower ramp rate of 2 °C/min from 240 °C until the completion of the $Ni_{1-x}Pt_xSi$ growth. During annealing, RBS data

a)e-mail: Jelle.Demeulemeester@fys.kuleuven.be

were acquired with a 2 MeV He-beam of 50–75 nA at a backscattering angle of 165°. The sample normal was tilted at an angle of 35° with respect to the incident beam, to enhance depth resolution. Every 2 min, an RBS spectrum was assembled, which results in a temperature resolution of 4 °C during the solid-phase reaction.

RBS is a powerful and well established technique in thin film research. It is fully quantitative in composition analysis and resolves depth information with a sensitivity of a few nanometers. Moreover, the quadratic increase in sensitivity to heavy target elements renders RBS extremely suitable to investigate the involvement of small quantities of Pt in the Ni silicide solid-phase reaction. Performing RBS *in situ* in real time thus allows to accurately probe the full atomic diffusion process, whereas the depth sensitivity enables to probe the thickness evolution of the growing and shrinking phases as a function of the annealing. Hence, real-time RBS is in principle well suited for dedicated kinetic studies. However, real-time RBS is not conventionally used to disentangle the growth kinetics since it requires a time-consuming analysis of a vast amount of RBS spectra (i.e., typically several hundreds per real-time RBS experiment). More conventional techniques such as real-time sheet resistance or real-time XRD provide a much less time-consuming way of extracting the kinetics parameters for simple thin film growth mechanisms. On the other hand, these methods — in contrast to real-time RBS — rely on an indirect relation with the grown thickness and lack the elemental and depth sensitivity of RBS. This could render the kinetic analysis ambiguous or even virtually impossible to interpret since other effects have to be taken into account. To investigate the growth kinetics in complex growth mechanisms, e.g., ternary systems such as Ni(Pt) silicide growth, one thus benefits of having access to the direct thickness versus annealing temperature or annealing duration, readily available via real-time RBS, to yield a reliable analysis.

Recently, groundbreaking progress has been achieved in real-time RBS by applying artificial neural networks (ANNs) to the data analysis.[17] This approach is based on pattern recognition and allows one to automatically link acquired RBS spectra to the quantitative information of interest, e.g., thickness of the growing or shrinking phases, stoichiometry, roughness, etc.[18] With this approach, huge RBS data sets can be analyzed quasi instantaneously, without deteriorating the quantitative accuracy. Once a network is trained to analyze RBS data on a specific type of system, the amount of spectra that can be analyzed is virtually unlimited, which makes real-time RBS much more appealing to apply in dedicated systematic investigations such as kinetic studies. Therefore, all RBS data were analyzed by an artificial neural network. The ANN results were visually checked by overlaying the NDF-simulation of the ANN output and the real data in an automated way.[19]

III. RESULTS

Real-time RBS data sets are conveniently displayed as contour plots. The real-time RBS contour plot of the pure Ni reference sample is shown in Fig. 1. Each horizontal slice in such a contour plot corresponds to a single RBS measurement captured at the temperature indicated at the y-axis. The x-axis represents the backscattering energy, whereas a color scale is used to represent the backscattering yield (z-axis). In Fig. 1, two main regions in backscattering energy, associated with the elemental distribution of Si and Ni, can be distinguished and are represented with an arrow. For each element, the highest backscattering energy (i.e., at the tail point of the arrow) corresponds to He-scattering from that specific element located at the sample surface. Lower backscattering energies correspond to scattering from atoms located deeper in the sample. Hence, the arrows directly represent a depth scale for Si and Ni.

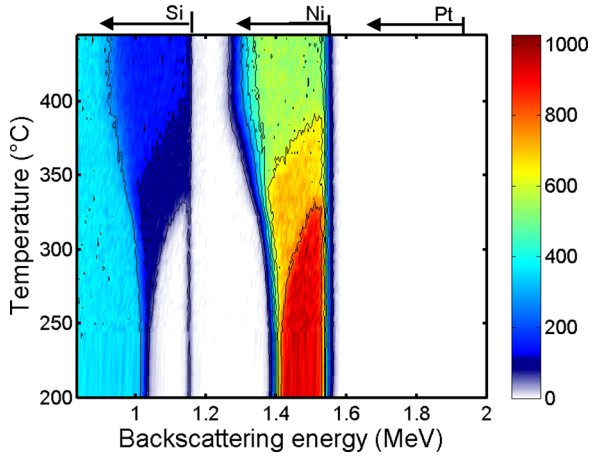

FIG. 1. Real-time RBS measurement on a 85 nm thin Ni film deposited on Si(100) and capped with 3 nm Si, performed during a ramped annealing at 2 °C/min. The elemental depth scales for Si, Ni, and Pt are added for the sake of clarity.

A transition of one phase to the next phase is visualized by a transition in color (backscattering yield) and bending contour lines. Those contour lines that separate the two color regions depict the position of the interface between the growing and the shrinking phase as a function of temperature. As such, the curvature of the contours is a measure for the growth rate. Two such phase transitions are seen in Fig. 1. The bending contour lines between 250 °C and 330 °C, both in the Si and the Ni signal, represent the growth of δ-Ni_2Si at the expense of Ni. The subsequent bending in contours between 330 °C and 390 °C is related to the transition of the fully grown δ-Ni_2Si layer to NiSi. Our results thus confirm the generally accepted Ni silicide formation sequence.[3] The transient crystalline transition from δ-Ni_2Si to θ is however not observed due to the similarity in stoichiometry of these phases and the fact that this transition requires merely local atomic rearrangement.[5]

The real-time RBS measurements on the alloyed films with Pt concentrations of 1, 3, 7, and 10 at. % are shown in Fig. 2. The Si and Ni signal in these contour plots show the same phase transitions as in the reference sample, i.e., Ni → δ-Ni_2Si and δ-Ni_2Si → NiSi. However, the systematic change in shape, curvature, and temperature window of these contours as a function of initial Pt concentration indicates that Pt has a large and systematic influence on the silicide growth kinetics, both for the Ni-rich silicide and for the

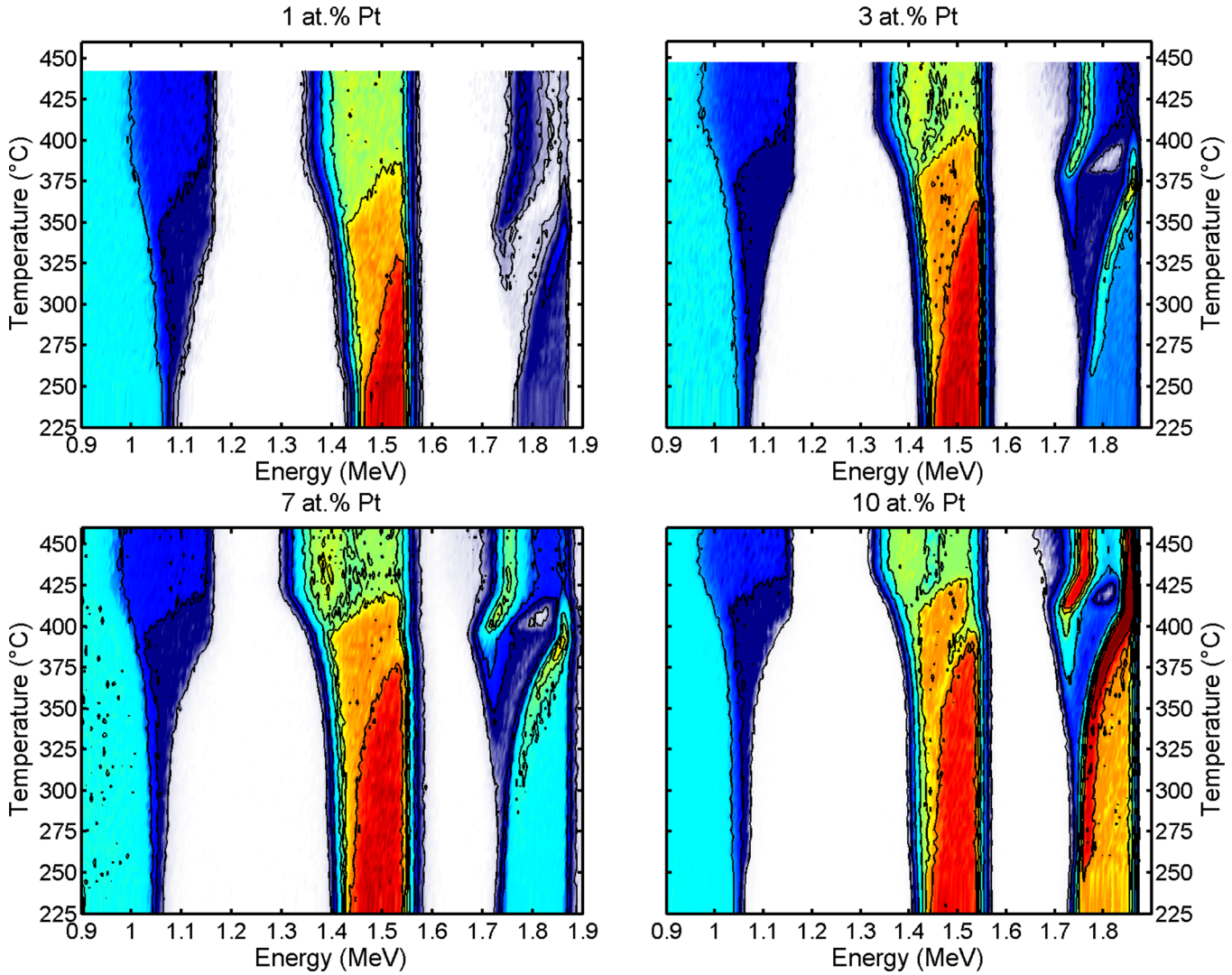

FIG. 2. Real-time RBS measurement on a 75 nm thin Ni film alloyed with 1, 3, 7, and 10 at. % Pt on Si(100), performed during a ramped annealing at 2 °C/min.

monosilicide growth. Additionally, these contour plots contain a third region at higher backscattering energies representing the Pt depth profile. It is clear from the complex Pt contour shapes that Pt redistributes in an erratic way during silicide formation. Pt is expelled towards the surface during δ-Ni_2Si formation, whereas Pt subsequently appears highly concentrated at the Si interface when the monosilicide starts to grow. This phenomenon can be assigned to the low solubility of Pt in δ-Ni_2Si compared to NiSi, and the high mobility of Pt in δ-Ni_2Si compared to pure Ni.[12] More detailed information on the established Pt redistribution profile during Ni(Pt) silicide formation can be found in Ref. 14.

In the following subsections, we will discuss the effect of Pt on the δ-Ni_2Si growth and on the $Ni_{1-x}Pt_xSi$ growth kinetics for which activation energies have been extracted as a function of the initial Pt concentration. These results are discussed and compared with literature in Sec. IV.

A. δ-Ni_2Si growth

In all of these real-time RBS measurements, δ-Ni_2Si is the first silicide phase observed to grow, irrespective of the Pt content, at least for Pt concentrations up to 10 at. %. It has been established in recent studies that this δ-Ni_2Si growth triggers a redistribution of the initially homogeneously distributed Pt.[20] Pt has a very limited solubility in the δ-Ni_2Si lattice and gets expelled at the Ni/δ-Ni_2Si interface as Ni atoms diffuse out of the as-deposited mixture to form δ-Ni_2Si. As such, a Pt-rich diffusion barrier for Ni gains thickness — and thus effectiveness — during the δ-Ni_2Si growth in a mechanism referred to as the snowplow effect.[15] Moreover, it has been observed by atom probe tomography that the majority of Pt embedded in the δ-Ni_2Si layer decorates the δ-Ni_2Si grain boundaries.[16] These grain boundaries comprise the dominating diffusion paths for Ni during δ-Ni_2Si growth.[21] An apparent small Pt content in the growing δ-Ni_2Si could thus have a fairly sizable effect on the δ-Ni_2Si growth kinetics, additionally to the effect of the growing Pt-rich diffusion barrier.

The effect of Pt on the δ-Ni_2Si growth kinetics is clearly observed in the real-time RBS measurements (Figs. 1 and 2). The shape and curvature of the contours characterizing the δ-Ni_2Si growth evidence a deceleration in δ-Ni_2Si growth kinetics, which is far more pronounced for increasing Pt

TABLE I. Overview of numbers that characterize the silicide growth as a function of Pt concentration. The temperature at which the Ni is fully consumed and the $Ni_{1-x}Pt_xSi$ phase is formed completely are shown in column T_{Ni} and T_{NiSi}, respectively. The last column lists the activation energies for the $Ni_{1-x}Pt_xSi$ growth, for which the activation energies obtained at a slower ramp rate of 1 °C/min are indicated with an asterisk.

	T_{Ni} (°C)	T_{NiSi} (°C)	E_a (eV)
0 at. % Pt	334	400	1.34 ± 0.06
1 at. % Pt	344	400	1.6 ± 0.5
			$^{*}1.8 \pm 0.1$
3 at. % Pt	373	412	2.9 ± 0.4
			$^{*}2.7 \pm 0.2$
7 at. % Pt	392	423	2.9 ± 0.5
10 at. % Pt	408	428	3.1 ± 0.5

concentrations. The slowed down δ-Ni_2Si growth kinetics result obviously in a shift of the temperature at which the Ni is completely consumed to higher temperatures for increasing Pt concentrations, whereas the onset temperature of δ-Ni_2Si growth remains the same for each Pt concentration. These values for the Ni consumption temperature are listed in Table I as a function of initial Pt concentration to give a quantitative estimate of the effect of Pt on the δ-Ni_2Si growth kinetics. Incorporating 10 at. % Pt in the Ni film thus delays the Ni consumption temperature from 334 °C to 408 °C when applying a slow ramp rate of 2 °C/min as a thermal treatment. It should be pointed out that the pure Ni sample has a slightly thicker Ni layer. A Ni film of the same thickness as the alloyed films would thus have completed δ-Ni_2Si growth at a temperature lower than 334 °C.

Recently, it has been shown that for an initial Pt concentration of 7 at. %, once a δ-Ni_2Si film of a certain thickness has grown, these Pt-induced slower growth kinetics result in the simultaneous growth of δ-Ni_2Si and monosilicide in the presence of an undepleted Ni reservoir.[14] In thin film binary diffusion couples, simultaneous growth of two phases is normally not observed unless the growing phase has exceeded a critical thickness before depletion of the metal reservoir.[22] In binary Ni/⟨Si⟩ thin film diffusion couples in particular, the δ-Ni_2Si critical thickness is so large that in practice it will not be reached. Annealing a thin Ni film on a Si substrate thus results in a sequential phase growth as observed in this real-time RBS measurement (Fig. 1). However, restricting the supply of one of the diffusing species can lower the critical thickness sufficiently to allow simultaneous growth, even in a thin film solid phase reaction.[23] In this study, we have observed the simultaneous growth of δ-Ni_2Si and NiSi for initial Pt concentrations as low as 1 at. %. This further indicates that the presence of Pt at the δ-Ni_2Si grain boundaries and Ni/δ-Ni_2Si interface could be a huge impediment to Ni diffusion.

Because of the many simultaneously ongoing processes (e.g., growth of δ-Ni_2Si, expulsion of Pt during δ-Ni_2Si growth, and growth of $Ni_{1-x}Pt_xSi$), it is virtually impossible to unambiguously obtain or interpret extracted activation energies. Therefore, activation energies for the growth of δ-Ni_2Si were omitted for this paper.

B. Monosilicide growth

The monosilicide phase is denoted as $Ni_{1-x}Pt_xSi$ since the Pt concentration varies as a function of depth throughout the solid-phase reaction. For each of the Pt concentrations, the $Ni_{1-x}Pt_xSi$ layer was observed to grow in two stages, in agreement with the growth model suggested in Ref. 14 as described below. First, a thin Pt-rich monosilicide seed layer grows simultaneously with δ-Ni_2Si before the depletion of the Ni reservoir (as mentioned above). Once the Ni reservoir is depleted $Ni_{1-x}Pt_x$, Si commences to grow at two fronts. (i) δ-Ni_2Si dissolves as δ-$Ni_2Si \rightarrow NiSi + Ni$ at the δ-Ni_2Si/$Ni_{1-x}Pt_xSi$ interface. The freshly formed monosilicide can directly incorporate the small amounts of Pt that were present in the δ-Ni_2Si and thus form $Ni_{1-x}Pt_xSi$ with a moderate Pt concentration on top of the Pt-rich monosilicide seed layer. (ii) At the same time, Ni released from the δ-Ni_2Si dissociation diffuses to the Si interface to form monosilicide at the Si interface. Due to limited diffusion of Pt in $Ni_{1-x}Pt_xSi$, this interface layer contains an extremely low Pt concentration. The growing $Ni_{1-x}Pt_xSi$ layer thus contains 3 regions with a different Pt concentration: (1) a region with a very low Pt concentration at the Si interface, (2) a Pt-rich region originating from the seed layer in the middle, and (3) a $Ni_{1-x}Pt_xSi$ region with a moderate concentration above the Pt-rich region. However, we want to emphasize that these three monosilicide regions cannot be seen as physically separated layers. They comprise a single $Ni_{1-x}Pt_xSi$ layer with three distinct regions in Pt concentration.

Full quantitative analysis of the RBS spectra however requires to include three $Ni_{1-x}Pt_xSi$ layers with variable Pt concentration in the simulation to enable fitting of the spectra. Such an analysis of a full real-time RBS measurement (the 7 at. % Pt sample ramped at 2 °C/min was taken as an example) by artificial neural networks is displayed in Fig. 3. At lower temperatures, the ANN analysis reveals the thickness as a function of temperature, for the shrinking Ni and the growing δ-Ni_2Si layer, respectively. At 350 °C, the monosilicide seed layer ($Ni_{1-x}Pt_xSi$ (2) in Fig. 3) starts to

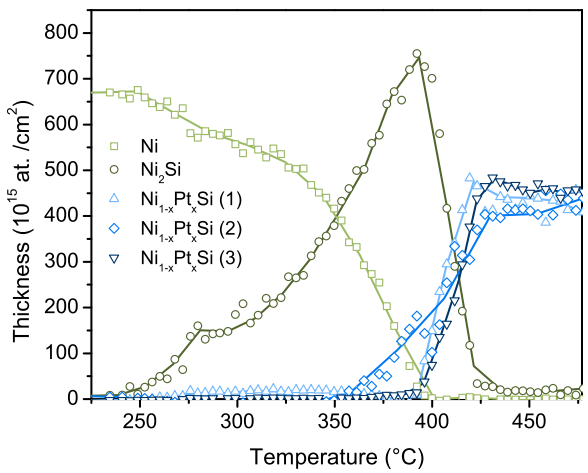

FIG. 3. Artificial neural network analysis of the real-time RBS measurement on the 7 at. % Pt alloy, performed at a ramp rate of 2 °C/min. The thickness of the Ni (squares), δ-Ni_2Si (circles), and three $Ni_{1-x}Pt_xSi$ regions (triangles, diamonds, and reversed triangles) are displayed as a function of annealing temperature.

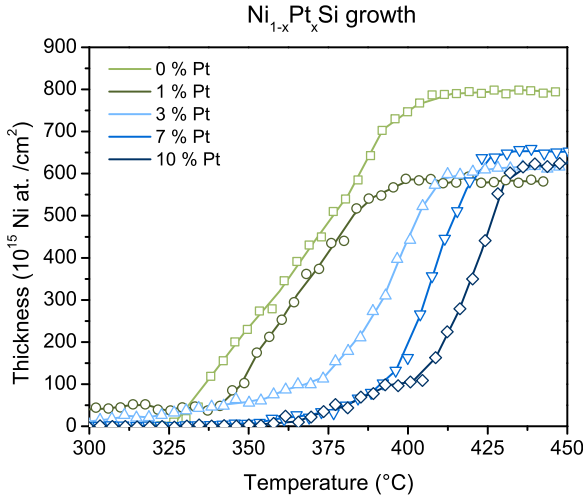

FIG. 4. Overview of the thickness evolution of the total $Ni_{1-x}Pt_xSi$ layer during 2 °C/min ramped real-time RBS measurements of Ni(Pt) alloy thin films on Si(100) containing 0 (squares), 1 (circles), 3 (triangles), 7 (reversed triangles), and 10 (diamonds) at. % Pt.

grow simultaneously with δ-Ni_2Si. Once the Ni reservoir is depleted at 392 °C, the much faster formation of $Ni_{1-x}Pt_xSi$ at two fronts commences. The $Ni_{1-x}Pt_xSi$ region moderate in Pt concentration ($Ni_{1-x}Pt_xSi$ (1) in Fig. 3) grows clearly at an equal pace as the Pt deficient $Ni_{1-x}Pt_xSi$ region ($Ni_{1-x}Pt_xSi$ (3) in Fig. 3) at the Si interface, as one would expect from the suggested growth model. The ANN results on the thickness of those three $Ni_{1-x}Pt_xSi$ regions were summed up to the total $Ni_{1-x}Pt_xSi$ thickness to perform the kinetics studies. An overview of the total $Ni_{1-x}Pt_xSi$ thickness evolution during the 2 °C/min ramped annealings is displayed in Fig. 4 for all studied Pt concentrations. The temperatures at which the $Ni_{1-x}Pt_xSi$ growth is completed are listed in Table I.

Figure 4 shows how the onset of this bulk $Ni_{1-x}Pt_xSi$ growth is delayed towards higher temperatures as a function of Pt concentration. This is most probably a direct consequence of the decelerated δ-Ni_2Si growth for increasing Pt concentrations. The temperatures of the depletion of the Ni reservoir listed in Table I can be taken as onset temperatures for the bulk of the $Ni_{1-x}Pt_xSi$ growth. Since there is a large scattering on the formation temperatures of this phase, it is no longer evident to study the effect of Pt on the $Ni_{1-x}Pt_xSi$ growth kinetics by comparing the growth rates. To understand how Pt addition influences the $Ni_{1-x}Pt_xSi$ growth kinetics, it is essential to extract the apparent activation energies as a function of the initial Pt concentration.

1. Extraction of activation energies E_a

Binary NiSi thin film growth is classified in literature as diffusion controlled growth. In a diffusion controlled growth mechanism, the square of the thickness is proportional to time $L^2 \simeq Dt$ when an isothermal annealing is applied, with D the diffusion coefficient. When dealing with diffusion controlled growth — also known as *parabolic growth* — activation energies (E_a) characterizing the growth kinetics are often assessed via ramped annealings and subsequent Kissinger analysis, or via isothermal annealings and the construction of an Arrhenius plot.[24] Both approaches are not restricted to a single technique and merely require the measurement of a quantity related to the thickness of the growing film, such as done in real-time x-ray diffraction[25] or real-time sheet resistance measurements.[26]

However, the direct thickness information readily available from the ANN analysis of a single real-time RBS measurement enables one to extract the activation energy by fitting the following equation to a plot of the squared thickness versus temperature:[27]

$$x^2 = x_0^2 + 2\frac{pn}{pn-mq}\frac{(m+n)^2}{mn}\frac{|\Delta H^R_{NiSi}|}{k_B}\frac{D_0}{\varphi}\int_{T_0}^{T}\frac{\exp\left(-\frac{E_a}{k_B}\right)}{T}dT. \quad (1)$$

This formula, describing the growth process during a ramped annealing at ramp rate φ, is directly derived from the Nernst-Einstein relation for diffusion driven by a chemical potential.[28] D_0 is defined as the pre-exponential factor, E_a is the activation energy, k_B is Boltzmann's constant, ΔH^R_{NiSi} is the reaction enthalpy, and p, n, m, and q depend on the stoichiometry of the reaction via $mA_pB_q + (pn - mq)B \rightarrow pA_mB_n$.

In principle, a non-linear least square fitting of Eq. (1) through the data is sufficient to obtain a good initial estimate of D_0 and E_a. However, the fitting algorithm can easily get trapped in local minima while moving E_a and D_0 through parameter space, which results in a seemingly good fit but incorrect values for the activation energy and pre-exponential coefficient. Therefore, the sum of the squared errors between the data and the fitting function (a figure of merit for the *goodness* of the fit) should be calculated as a function of the two parameters, E_a and D_0. The *goodness* of these fits, displayed as a contour plot in a grid of E_a and D_0, allows to determine the global minimum and thus the correct kinetic parameters. Such a contour plot obtained during the grid-search fitting of the NiSi growth in the binary diffusion couple is shown in Fig. 5. The grid-plot clearly reveals the presence of various local minima that could yield a seemingly good fit. An overview of the grid-search fits through the data acquired during the 2 °C/min ramps is shown in Fig. 6.

Note that the kinetic parameters obtained are only valid for the $Ni_{1-x}Pt_xSi$ growth once the Ni reservoir has been depleted. Preceding data points of the $Ni_{1-x}Pt_xSi$ thickness were not included in the fit. In this examined regime, only single phase growth is observed in contrast to the earlier stages where the $Ni_{1-x}Pt_xSi$ seed layer and the Ni-rich silicide phase are growing simultaneously. For all samples, it has been confirmed that the growth process is parabolic—and that Eq. (1) can be applied to extract the activation energy—by performing real-time RBS during an isothermal annealing an plotting the squared thickness as a function of annealing time (not shown).

2. $Ni_{1-x}Pt_xSi$ growth kinetics

The activation energies obtained are plotted in Fig. 7 along with the statistical error bars and are listed in Table I

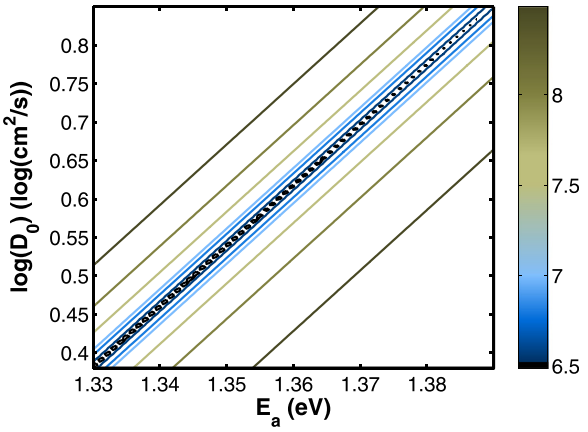

FIG. 5. Variance between the data on the growth of NiSi and the kinetic fits (using Eq. (1)) while moving E_a and D_0 through parameter space in a grid search. The data on the growth of the NiSi layer are extracted from real-time RBS during a ramped annealing at 2 °C/min of the Ni + 0 at. % Pt thin film on Si(100).

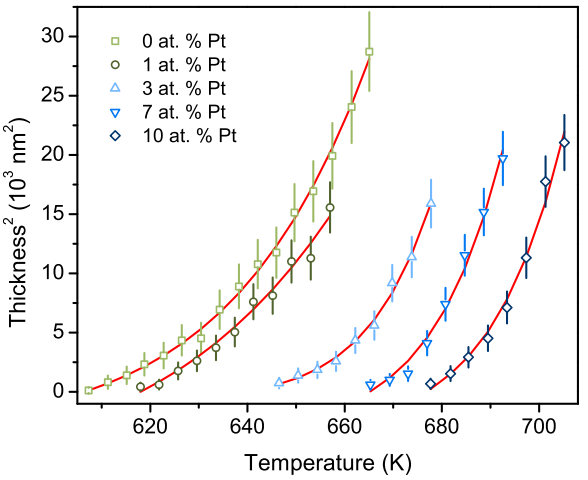

FIG. 6. Overview of the kinetic fits (using Eq. (1)), depicted by the red curves, to extract the activation energies for the $Ni_{1-x}Pt_xSi$ growth. The data on the growth of the $Ni_{1-x}Pt_xSi$ layer (data points) were obtained from real-time RBS during a ramped annealing at 2 °C/min.

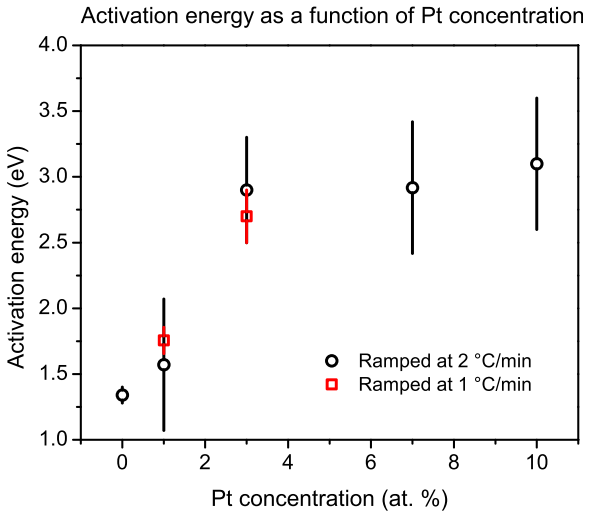

FIG. 7. Activation energies for $Ni_{1-x}Pt_xSi$ growth as a function of Pt concentration. The activation energies are extracted from annealing at a ramp rate of 2 °C/min (circles) or 1 °C/min (squares).

as a function of initial Pt concentration. To extract the activation energies, all samples were subjected to an identical 2 °C/min ramp (circles in Fig. 7), while an additional slower ramp at 1 °C/min was performed for the samples containing 1 and 3 at. % Pt (squares in Fig. 7). The variation in height of the error bars mainly arises from the different number of relevant data points available on the ramp for fitting. As such, the activation energies obtained for lower Pt concentrations or the 1 °C/min ramps in which $Ni_{1-x}Pt_xSi$ growth proceeds slower are more precise. The slower ramps confirm and further refine the results obtained from the 2 °C/min ramps.

Figure 7 illustrates that the activation energies for $Ni_{1-x}Pt_xSi$ growth clearly increase as a function of Pt concentrations between 0 and 3 at. %. Even a small Pt content of merely 1 at. % already induces an increase in activation energy from 1.34 eV to 1.8 eV, whereas including 3 at. % Pt raises the activation energy to a quite large value of 2.7 eV. Further increasing the Pt content to 7 or 10 at. % Pt does not result in a remarkable increase of E_a compared to 3 at. % Pt. Activation energies of 2.9 eV and 3.1 eV characterizing the $Ni_{1-x}Pt_xSi$ growth were determined for the 7 and 10 at. % samples, respectively.

IV. DISCUSSION

We have shown that fairly low Pt concentrations of 1 to 10 at. % exert a large effect on the δ-Ni_2Si growth kinetics. The δ-Ni_2Si growth is slowed down increasingly for larger Pt concentrations. It is suggested that this growth deceleration is achieved by the complex redistribution of Pt during δ-Ni_2Si formation, in which Pt appears highly concentrated in the Ni diffusion paths. (i) Pt is expelled and forms a diffusion barrier between the Ni supply and the growing δ-Ni_2Si phase[15] and (ii) Pt blocks the Ni diffusion paths in the δ-Ni_2Si grain boundaries (for which Ni diffusion has the largest diffusion coefficient in the pure Ni/Si systems).[16] The Pt-induced deceleration in δ-Ni_2Si growth in turn influences the subsequent $Ni_{1-x}Pt_xSi$ growth. First, $Ni_{1-x}Pt_xSi$ and δ-Ni_2Si are observed to grow simultaneously, which is most probably invoked by the hindered/limited Ni diffusion. Hence, a thin $Ni_{1-x}Pt_xSi$ seed layer is able to grow before the Ni reservoir is depleted, and the fast $Ni_{1-x}Pt_xSi$ single phase growth kicks in. Second, the slower δ-Ni_2Si growth shifts the point at which the Ni reservoir is depleted toward much higher temperatures. As a consequence, the onset temperature of the $Ni_{1-x}Pt_xSi$ single phase growth (which coincides with the temperature at which Ni is depleted) is delayed toward elevated temperatures for larger Pt concentrations.

It has been argued in literature that the more stable texture of $Ni_{1-x}Pt_xSi$ arises from a slight Pt-induced increase in lattice parameter, which steers the texture selection.[13] PtSi and NiSi share the same orthorhombic PnM prototype crystal structure, though with a larger lattice parameter for PtSi.[29] This renders Pt soluble in the NiSi phase and allows Pt to occupy Ni lattice sites to form the $Ni_{1-x}Pt_xSi$ phase with a slightly expanded lattice. Moreover, the fact that Pt appears highly concentrated in the NiSi seed layer during the initial stages of monosilicide growth further strengthens this idea.[12] On the other hand, recent findings by Mangelinck *et al.*[30] show

that the Pt content in the NiSi seed layer is prominently located at NiSi grain boundaries during the first stages. This could diminishes the argument that the reduced axiotaxial texture is a direct result of a Pt induced lattice expansion. Our results indicate that kinetic considerations should be taken into account as well. First, the slower δ-Ni_2Si growth kinetics imply that the bulk of the $Ni_{1-x}Pt_xSi$ growth starts at elevated temperatures (delayed by at least 74 °C) where lattice diffusion gains importance over the grain boundary diffusion in NiSi. Since lattice diffusion is highly anisotropic in NiSi, altered kinetics as such can promote the growth of different texture components at higher temperatures. Second, thin film agglomeration requires diffusion to reshape the grain envelope. This might require elevated temperatures due to reduced kinetics of Ni in $Ni_{1-x}Pt_xSi$. Additionally, Pt diffusion in the $Ni_{1-x}Pt_xSi$ phase requires largely elevated temperatures as well. This is clearly reflected in the inhomogeneous Pt profile in the $Ni_{1-x}Pt_xSi$ phase, which barely changes after 30 min of annealing at 600 °C.[14] This indicates that higher temperatures will be required to generate enough atomic mobility to initiate the agglomeration. Such an interplay between slower growth kinetics and an increased morphological stability was also found for NiSi in the presence of W, Ti, and Ta alloying elements.[31]

Furthermore, texture or interface energy is not the only parameter that influences the film stability against agglomeration upon high temperature annealing. The fact that the majority of the Pt is located in between the initial NiSi grains indicates that the addition of Pt can limit the lateral growth of the monosilicide grains. From a theoretical point of view, reducing the grain size/film thickness ratio is expected to induce a large decrease in the critical thickness above which no agglomeration can occur.[32] As such, a Pt induced reduction in $Ni_{1-x}Pt_xSi$ grain size could indeed yield agglomeration resistant $Ni_{1-x}Pt_xSi$ films down to a certain critical film thickness, lower than in the case of a pure $Ni/\langle Si\rangle$ system.

Activation energies for the $Ni_{1-x}Pt_xSi$ growth kinetics have not been reported yet. However, we can compare our findings on the growth kinetics for pure NiSi to literature values. These reported activation energies vary between 1.2 – 1.8 eV.[3,33–35] Our extracted activation energy for NiSi growth ($E_a = 1.35 \pm 0.06$ eV) thus agrees well with the lower range of activation energies. Colgan and d'Heurle however remarked that the apparent activation energy determined with the Kissinger method is usually larger than the values obtained from isothermal data and an Arrhenius plot.[36] They argued that the initial linear growth of the thin film is filtered out in isothermal annealing and not in the Kissinger method, which relies on ramped annealings. In that respect, it is thus obvious that E_a values obtained via our method, where the direct thickness information is used and the first data points are excluded from the fitting, result in lower apparent activation energies compared to values obtained from Kissinger analysis. Moreover, our results are in agreement with isothermal data, i.e., 1.23 eV.[34]

The observed trend of an increase in activation energies for larger Pt concentrations up to 3 at % is clearly visible. The activation energy for $Ni_{1-x}Pt_xSi$ growth is increased from $E_a = 1.35 \pm 0.06$ eV to $E_a = 2.7 \pm 0.2$ eV for 3 at. % Pt, which is a rather large increase of 1.35 eV. This increase can be related to many factors, such as (i) a change in the relative importance of grain boundary diffusion over lattice diffusion or (ii) a change in activation energies for both individual diffusion mechanism.

With respect to the diffusion mechanism, delaying a solid phase reaction to higher temperatures (which is the case) can alter the diffusion mechanism by enhancing the role of lattice diffusion, over grain boundary diffusion. Lattice diffusion is usually characterized by a larger activation energy, leading to a larger overall activation energy for the combined diffusion mechanism. Additionally, there is an indication that the high Pt content in the initial monosilicide seed layer limits the lateral grain growth, and thus reduces the size of the $Ni_{1-x}Pt_xSi$ grains.[30] Increasing the initial Pt concentration could thus alter the relative densities of the grain boundary and lattice diffusion paths in the monosilicide. However, from this type of experiments, it is impossible to decouple lattice diffusion from grain boundary diffusion in order to study the influence of Pt on either mechanism.

On the other hand, Pt could also influence the individual activation energies for Ni diffusion in the lattice or grain boundaries. Pt might affect the activation energy by hampering the Ni diffusion from the shrinking Pt-containing δ-Ni_2Si layer. Ciccariello *et al.* for instance showed that the Ni grain boundary and lattice self-diffusion in δ-Ni_2Si play a major role in the growth of the monosilicide.[37] Since Pt resides mainly at the δ-Ni_2Si grain boundaries, Pt can influence the Ni supply to the growing monosilicide and increase the activation energy for Ni diffusion. Moreover, Pt at the $Ni_{1-x}Pt_xSi$ grain boundaries, or in the $Ni_{1-x}Pt_xSi$ phase itself, might obstruct the Ni grain boundary diffusion or lattice diffusion respectively, causing an extra increase in activation energy. Hence the increase in activation energy for monosilicide growth most probably originates from a complex interplay between several Pt-induced effects.

Further increasing the initial Pt content from 3 at. % to 7 or 10 at. % Pt merely results in a larger activation energy, taking the error bars into account. This suggests that for initial Pt concentrations above 3 at. %, saturation effects are involved. Detailed analysis of the individual RBS spectra reveals that the amount of Pt that gets expelled during the δ-Ni_2Si growth is much larger for higher initial Pt concentrations. Once the Ni has diffused completely through this diffusion barrier and the fast $Ni_{1-x}Pt_xSi$ single phase growth can actually start, the expelled Pt is located at the surface. It is thus suggested that the expelled Pt cannot effectively influence the diffusion processes at the reaction interface. Thus, increasing the initial Pt concentration above 3 at. % does not result in a remarkable increase of the Pt content effectively present at the reaction interface. The diffusion process and consequently the activation energy thus remain basically unaffected. It does, however, still delay the onset temperature of the $Ni_{1-x}Pt_xSi$ single phase growth slightly by increasingly slowing down the δ-Ni_2Si growth for higher initial Pt concentrations.

V. CONCLUSIONS

Real-time RBS in combination with artificial neural network analysis was successfully applied to disentangle the

growth kinetics during the complex growth of Ni(Pt) silicides. We showed that activation energies can be extracted from a single ramped real-time RBS measurement. Small additions of Pt clearly have a huge effect on the δ-Ni_2Si growth kinetics. Simultaneous growth of $Ni_{1-x}Pt_xSi$ and δ-Ni_2Si is observed because of the limited Ni diffusion — even for initial Pt concentrations as low as 1 at. %. Additionally, the temperature of Ni depletion is shifted towards elevated temperatures for larger Pt concentrations because of the slower δ-Ni_2Si growth kinetics. This consequently delays $Ni_{1-x}Pt_xSi$ growth to higher temperatures as well.

The activation energies for the $Ni_{1-x}Pt_xSi$ growth were observed to increase from $E_a = 1.35 \pm 0.06$ eV for pure NiSi to $E_a = 2.7 \pm 0.2$ eV for 3 at. % Pt. A possible explanation for the large increase in activation energy is that Ni diffusion is hampered by Pt residing along the diffusion paths. Alternatively, the delay towards elevated temperatures could increase the contribution of lattice diffusion in the monosilicide, which is usually characterized by a larger activation energy than that of grain boundary diffusion. Above 3 at. % Pt, the increase in activation energy stalls and reaches $E_a = 3.1 \pm 0.5$ eV for 10 at. % Pt. The saturation effect is attributed to the fact that initial Pt concentrations above 3 at. % do not result in a remarkable increase of the Pt content that effectively takes part of the $Ni_{1-x}Pt_xSi$ formation.

ACKNOWLEDGMENTS

This work was supported by the Fund for Scientific Research, Flanders (FWO), the Concerted Action Programs (GOA/2009/006 and GOA/2014/007) of the KULeuven, the National Research Foundation (South Africa) and SPIRIT (contract no. 227012). The authors also wish to thank the Material Research Group at iThemba LABS for the use of their facilities.

[1]S.-L. Zhang and M. Östling, Crit. Rev. Solid State Mater. Sci. **28**, 1 (2003).
[2]C. Lavoie, F. M. d'Heurle, C. Detavernier, and C. Cabral, Jr., Microelectron. Eng. **70**, 144 (2003).
[3]F. d'Heurle, C. S. Petersson, J. E. E. Baglin, S. J. La Placa, and C. Y. Wong, J. Appl. Phys. **55**, 4208 (1984).
[4]F. M. d'Heurle and C. S. Petersson, Thin Solid Films **128**, 283 (1985).
[5]S. Gaudet, C. Coia, P. Desjardins, and C. Lavoie, J. Appl. Phys. **107**, 093515 (2010).
[6]W. K. Chu, H. Kratle, J. W. Mayer, H. Müller, M.-A. Nicolet, and K. N. Tu, Appl. Phys. Lett. **25**, 454 (1974).
[7]R. Pretorious, C. L. Ramiller, S. S. Lau, and M.-A. Nicolet, Appl. Phys. Lett. **30**, 501 (1977).
[8]T. Finstad, Phys. Status Solidi A **63**, 223 (1981).
[9]C. Lavoie, C. Detavernier, C. Cabral, Jr., F. M. d'Heurle, A. J. Kellock, J. Jordan-Sweet, and J. M. E. Harper, Microelectron. Eng. **83**, 2042 (2006).
[10]D. Mangelinck, J. Y. Dai, J. S. Pan, and S. K. Lahiri, Appl. Phys. Lett. **75**, 1736 (1999).
[11]J. F. Liu, H. B. Chen, J. Y. Feng, and J. Zhu, Appl. Phys. Lett. **77**, 2177 (2000).
[12]J. Demeulemeester, D. Smeets, C. Van Bockstael, C. Detavernier, C. M. Comrie, N. P. Barradas, A. Vieira, and A. Vantomme, Appl. Phys. Lett. **93**, 261912 (2008).
[13]C. Detavernier and C. Lavoie, Appl. Phys. Lett. **84**, 3549 (2004).
[14]J. Demeulemeester, D. Smeets, C. Comrie, C. Van Bockstael, C. Detavernier, K. Temst, and A. Vantomme, J. Appl. Phys. **108**, 043505 (2010).
[15]O. Cojocaru-Mirédin, D. Mangelinck, K. Hoummada, E. Cadel, D. Blavette, B. Deconihout, and C. Perrin-Pellegrino, Scr. Mater. **57**, 373 (2007).
[16]B. Imbert, C. Guichet, S. Bonnetier, S. Zoll, M. Juhel, M. Hopstaken, P. Clifton, and O. Thomas, Microelectron. Eng. **84**, 2523 (2007).
[17]J. Demeulemeester, D. Smeets, N. P. Barradas, C. M. Comrie, A. Vieira, K. Temst, and A. Vantomme, Nucl. Instrum. Methods B **268**, 1676 (2010).
[18]N. P. Barradas and A. Vieira, Phys. Rev. E **62**, 5818 (2000).
[19]N. P. Barradas, C. Jeynes, and R. P. Webb, Appl. Phys. Lett. **71**, 291 (1997).
[20]K. Hoummada, C. Perrin-Pellegrino, and D. Mangelinck, J. Appl. Phys. **106**, 063511 (2009).
[21]J. E. E. Baglin, H. A. Atwater, D. Gupta, and F. M. d'Heurle, Thin Solid Films **93**, 255 (1982).
[22]U. Gösele and K. N. Tu, J. Appl. Phys. **53**, 3252 (1982).
[23]A. Vantomme, M.-A. Nicolet, and N. D. Theodore, J. Appl. Phys. **75**, 3882 (1994).
[24]H. E. Kissinger, Anal. Chem. **29**, 1702 (1957).
[25]W. Knaepen, C. Detavernier, R. L. Van Meirhaeghe, J. J. Sweet, and C. Lavoie, Thin Solid Films **516**, 4946 (2008).
[26]S.-L. Zhang and F. M. d'Heurle, Thin Solid Films **256**, 155 (1995).
[27]C. C. Theron, J. C. Lombard, and R. Pretorious, Nucl. Instrum. Methods B **161**, 48 (2000).
[28]A. Einstein, Ann. Phys. **322**, 549 (1905).
[29]*Properties of Metal Silicides*, edited by K. Maex and M. Van Rossum (INSPEC, the Institution of Electrical Engineers, London, United Kingdom, 1995), p. 14.
[30]D. Mangelinck, K. Hoummada, A. Portavoce, C. Perrin, R. Daineche, M. Descoins, D. J. Larson, and P. H. Clifton, Scr. Mater. **62**, 568 (2010).
[31]D. Deduytsche, C. Detavernier, R. L. Van Meirhaeghe, J. L. Jordan-Sweet, and C. Lavoie, J. Appl. Phys. **101**, 044508 (2007).
[32]T. P. Nolan, R. Sinclair, and R. Beyers, J. Appl. Phys. **71**, 720 (1992).
[33]C.-D. Lien, M.-A. Nicolet, and S. S. Lau, Thin Solid Films **143**, 63 (1986).
[34]G. Majini, F. Della Valle, and C. Nobili, J. Phys. D: Appl. Phys. **17**, L77 (1984).
[35]D. M. Scott and M-A. Nicolet, Phys. Status Solidi A **66**, 773 (1981).
[36]E. G. Colgan and F. M. d'Heurle, J. Appl. Phys. **79**, 4087 (1996).
[37]J. C. Ciccariello, S. Poize, and P. Gas, J. Appl. Phys. **67**, 3315 (1990).